

# Modeling the Impact of Phase Noise on the Performance of Crystal-Free Radios

Osama Khan, Brad Wheeler, Filip Maksimovic, David Burnett, Ali M. Niknejad, and Kris Pister

**Abstract**—We propose a crystal-free radio receiver exploiting a free-running oscillator as a local oscillator (LO) while simultaneously satisfying the 1% packet error rate (PER) specification of the IEEE 802.15.4 standard. This results in significant power savings for wireless communication in millimeter-scale microsystems targeting Internet of Things applications. A discrete time simulation method is presented that accurately captures the phase noise (PN) of a free-running oscillator used as an LO in a crystal-free radio receiver. This model is then used to quantify the impact of LO PN on the communication system performance of the IEEE 802.15.4 standard compliant receiver. It is found that the equivalent signal-to-noise ratio is limited to  $\sim 8$  dB for a  $75\text{-}\mu\text{W}$  ring oscillator PN profile and to  $\sim 10$  dB for a  $240\text{-}\mu\text{W}$  LC oscillator PN profile in an AWGN channel satisfying the standard's 1% PER specification.

**Index Terms**—Crystal-free radio, discrete time phase noise modeling, free-running oscillators, IEEE 802.15.4, incoherent matched filter, Internet of Things (IoT), low-power radio, minimum shift keying (MSK) modulation, O-QPSK modulation, power law noise, quartz crystal (XTAL), wireless communication.

## I. INTRODUCTION

ECONOMIES of scale require the millimeter-scale wireless sensing systems that form the foundation of the Internet of Things (IoT) to be low-cost and energy autonomous. This vision is driving complete system integration on a single piece of silicon to improve the system energy efficiency for continuous operation on harvested energy and to reduce cost.

Almost all commercial microsystems today rely on off-chip quartz technology for precise timing and frequency reference. The quartz crystal (XTAL) is a bulky off-chip component that

Manuscript received August 26, 2016; accepted September 11, 2016. Date of publication September 20, 2016; date of current version June 23, 2017. This work was supported in part by the DARPA Vanishing Programmable Resources (VAPR) Program, in part by the Berkeley Wireless Research Center, in part by the National Science Foundation Graduate Research Fellowship under Grant 1106400, and in part by the Morphing Autonomous Gigascale Integrated Circuits (MAGIC) under Grant DARPA-BAA-13-23. This brief was recommended by Associate Editor F. C. M. Lau.

O. Khan, B. Wheeler, F. Maksimovic, D. Burnett, and K. Pister are with Berkeley Sensor and Actuator Center, University of California at Berkeley, Berkeley, CA 94720 USA (e-mail: oukhan@berkeley.edu; brad.wheeler@berkeley.edu; fil@berkeley.edu; db@berkeley.edu; ksjp@berkeley.edu).

A. M. Niknejad is with the Berkeley Wireless Research Center, University of California at Berkeley, Berkeley, CA 94720 USA (e-mail: niknejad@berkeley.edu).

Color versions of one or more of the figures in this paper are available online at <http://ieeexplore.ieee.org>.

Digital Object Identifier 10.1109/TCSII.2016.2611643

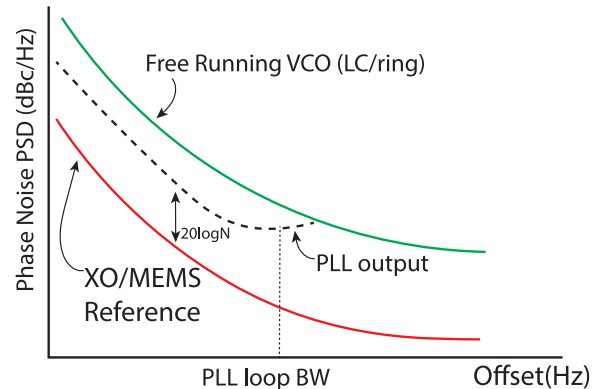


Fig. 1. Typical PN plot of an RF oscillator locked to a stable crystal frequency reference.

puts a size limitation on miniaturization and adds to the bill of material cost of a sensor node.

Alternatively, MEMS technology is showing promising results for replacing the XTAL in commercial products in space-constrained applications [1], [2]. However, it is still an off-chip frequency reference and the packaging adds to the cost of a sensor node. Attempts have been made to generate a precise on-chip frequency reference using calibration techniques [3], [4]. But the achieved accuracy is still insufficient to satisfy stringent wireless standards specification for low-power radios, e.g., BLE/IEEE 802.15.4. In contrast, we have presented a network level solution that allows a crystal-free sensor node to derive an accurate time and frequency reference in the absence of an off-chip frequency reference (XTAL) [5]. In this brief, we specifically address the impact of phase noise (PN) on the communication system performance of a crystal-free radio.

In a traditional radio architecture the RF oscillator (LC/ring) is locked in a phase locked loop (PLL) to a stable crystal frequency reference (XO) to improve the close-to-carrier PN which determines the long-term frequency drift of an oscillator (excluding environmental and aging effects) as shown conceptually in Fig. 1. In the absence of a stable XO, the free-running RF oscillator is tuned to operate at the desired RF channel frequency using a network calibrated on-chip frequency reference (see Fig. 2). Then the error in the desired RF channel frequency will be determined by the accuracy of the on-chip frequency reference [5]. The noisy local oscillator (LO) in the architecture proposed in Fig. 2 is operating open-loop as a frequency calibrated free-running RF oscillator and therefore the

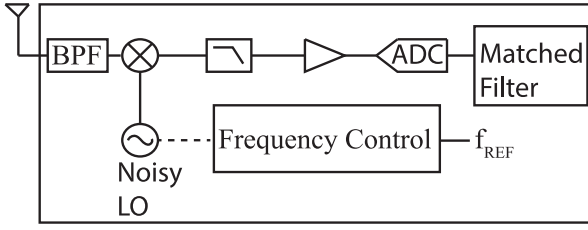


Fig. 2. Free-running RF oscillator used as an LO.

impact of its PN on the communication system performance needs to be carefully evaluated.

To accurately model a free-running oscillator, one has to model the power law noise that is nonstationary and difficult to analyze analytically [6]. In this brief, we resort to numerical simulation and present a discrete-time simulation model for the power law noise that accurately captures the close-in PN of a free-running oscillator. This model is then used to quantify its impact on the communication system performance of an IEEE 802.15.4 standard compliant radio receiver. An effort is made to provide a summary of the relevant equations and a discrete-time simulation model is presented that is cross-validated with foundry computer-aided design models of an RF oscillator.

## II. POWER LAW NOISE

Consider a sinusoidal oscillator signal  $v(t)$  with a nominal oscillation frequency  $f_o$  Hz

$$v(t) = [A + a(t)] \cos[2\pi f_o t + \phi(t)] \quad (1)$$

where  $A$  is the mean amplitude,  $a(t)$  is the zero-mean amplitude modulation (AM) noise and  $\phi(t)$  contains all phase and frequency errors from the nominal oscillation frequency  $f_o$  and phase  $2\pi f_o t$ . Phase disturbance  $\phi(t)$  includes random zero-mean phase modulation noise, initial phase and integrated effects of frequency offset and drift [6]. Oscillators contain an amplitude control mechanism that suppresses AM noise and it is therefore usually neglected.

PN  $\phi(t)$  is characterized in the frequency domain. The random PN  $\phi(t)$  spreads the spectrum of an ideal sinusoid in the frequency domain which otherwise is a Dirac-delta function. It is important to distinguish between a pass-band spectrum  $P_{RF}(f)$  of an oscillator which is a Fourier transform of  $v(t)$  from the baseband noise spectrum which is a Fourier transform of the autocorrelation of  $\phi(t)$  and is known as phase spectral density  $S_{\text{phi}}(f)$  with units  $\text{rad}^2/\text{Hz}$ . The phase spectral density  $S_{\text{phi}}(f)$  is a frequency domain measure of PN. Empirical measurements have shown that the  $S_{\text{phi}}(f)$  can be well approximated by [6]

$$S_{\text{phi}}(f) \approx \frac{h_4}{f^4} + \frac{h_3}{f^3} + \frac{h_2}{f^2} + \frac{h_1}{f^1} + h_0 \quad (2)$$

where the  $h_x$  are coefficients that are oscillator specific and the power  $x$  models a particular noise process. There are five distinct noise processes, which are called the power-law noise processes. A particular oscillator may not contain all of the five noise processes. On a log-log plot each noise process has

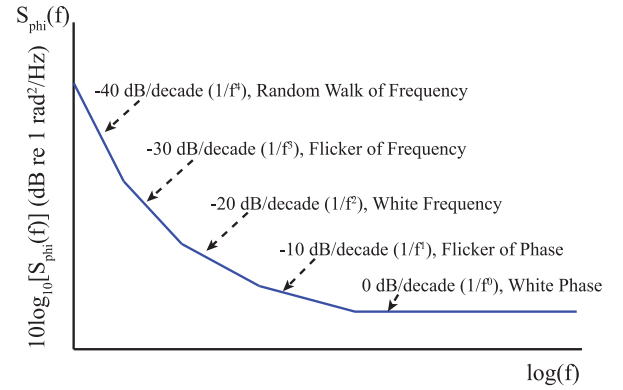


Fig. 3. Phase spectral density plot for power law noise [7].

a unique slope as shown in Fig. 3 [7]. The y-axis unit on a log scale is decibel relative to  $1 \text{ rad}^2/\text{Hz}$  [6].

The fractional frequency deviation  $y(t)$  of an oscillator is defined as [8]

$$y(t) = \frac{1}{2\pi f_o} \frac{\partial \theta(t)}{\partial t}. \quad (3)$$

The spectral density  $S_y(f)$  of fractional frequency deviation  $y(t)$  is related to the phase spectral density  $S_{\text{phi}}(f)$  as

$$S_y(f) = \left(\frac{f}{f_o}\right)^2 S_{\text{phi}}(f). \quad (4)$$

The  $S_{\text{phi}}(f)$  or  $S_y(f)$  characterizes the power law noise in the frequency domain. In the time-domain, due to the nonstationary nature of the power law noise, several statistical measures have been defined to estimate the frequency stability of an oscillator. One widely used measure to estimate frequency stability is the Allan variance defined as [7], [9]

$$\sigma_y^2(\tau) = \frac{1}{2(M-1)} \sum_{k=1}^{M-1} (\bar{y}_{k+1} - \bar{y}_k)^2 \quad (5)$$

where  $\bar{y}_k$  are the  $M$  average fractional frequency measurements with zero dead-time and  $\tau$  is the frequency measurement time interval [7].

The measurement interval  $\tau$  over which the frequency is averaged acts as a low-pass transfer function while the differencing operation between two successive fractional frequency measurements acts as a high-pass transfer function in the frequency domain [10]. Therefore the transfer function that relates the time-domain Allan variance with frequency-domain PN spectral density measurement  $S_{\text{phi}}(f)$  has a band-pass characteristic and is given by [8]

$$\sigma_y^2(\tau) = 2 \int_{f_l}^{f_h} \left(\frac{f}{f_o}\right)^2 S_{\text{phi}}(f) \frac{\sin^4(\pi f \tau)}{(\pi f \tau)^2} df. \quad (6)$$

The lower limit of integration  $f_l$  is approximated by the reciprocal of the total measurement time of interest while the upper limit of integration  $f_h$  is determined by the bandwidth of the oscillator circuit or the PN measurement instrument, which ever is smaller [6], [10]. Equation (6) is the link between the PN and the short-term frequency stability of an oscillator as measured by the Allan variance.

The on-chip (LC/ring) oscillators mainly exhibit the flicker and white frequency noise, therefore we will discuss a discrete time model for simulating these two noise types specifically. However, the model is general and able to simulate all of the five power law noise processes.

#### A. Discrete Time Model of White Frequency Noise

The white frequency ( $1/f^2$ ) noise process is modeled as an integral of white noise that is a Wiener random process also known as Brownian motion. The discrete PN simulation  $\Phi(n)$  of continuous time PN process  $\phi(t)$  modeling white frequency noise is given by [11], [12]

$$\phi(k) = 2\pi f_o \sum_{n=0}^{k-1} \sqrt{c\Delta t} w_n \quad (7)$$

where  $c$  is the constant that determines the rate at which the variance of an oscillator increases with time due to the white frequency noise [13],  $\Delta t$  is the simulation time-step, and  $w_n$  is the independent standard Gaussian random variable.

#### B. Discrete Time Model of Flicker of Frequency Noise

To correctly model the flicker of frequency noise ( $1/f^3$ ) or any colored noise, the generated noise sequence must satisfy the autocorrelation properties, causality, scale-invariance, have the proper Allan variance and the desired spectral density slope [14]. One such model was first proposed by Hosking [15] using fractional calculus and later utilized to generate the proper nonstationary noise sequences [14]. The discrete PN simulation  $\Phi(n)$  of continuous time PN process  $\phi(t)$  modeling flicker of frequency noise is given by [12], [14]

$$\phi(k) = 2\pi f_o \times \sqrt{2\pi c_F \Delta t} \sum_{n=0}^{k-1} h_{k-n} w_n \quad (8)$$

where  $c_F$  is the constant that determines the rate at which the variance of an oscillator increases with time due to the flicker of frequency noise and  $h_k$  is the impulse response that convolves the independent standard Gaussian random variable  $w_n$ . The impulse response is defined recursively as [14]

$$\begin{aligned} h_0 &= 1 \\ h_k &= \left(k - 1 - \frac{\beta}{2}\right) \frac{h_{k-1}}{k} \end{aligned} \quad (9)$$

where  $\beta = -x$ , e.g.,  $\beta = -3$  for flicker of frequency noise ( $1/f^3$ ).

#### C. Discrete Time Simulation of Free-Running Oscillator

The RF spectrum  $P_{RF}(f)$  of an oscillator in the presence of PN is characterized with one-sided RF spectral density

$$L(\Delta f) = \frac{P(f_o + \Delta f)}{P_{\text{Tot}}} \quad (10)$$

where  $L(\Delta f)$  is the noise power at an offset frequency of  $\Delta f$  from the carrier frequency of  $f_o$  in a 1 Hz bandwidth relative to the total power in the signal  $P_{\text{Tot}}$ . It is commonly expressed in

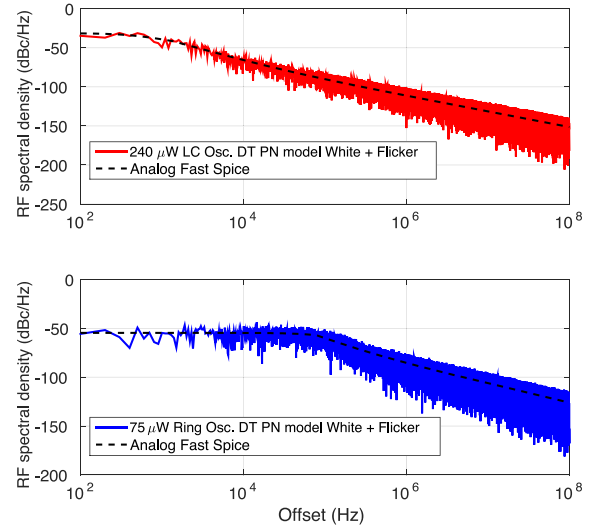


Fig. 4. Simulated RF spectral density of free-running oscillators.

decibel format as  $10\log_{10}[L(\Delta f)]$  dBc/Hz, where dBc means relative to the total power in the signal [6].

It is to be noted that  $\phi(t)$  is in general a nonstationary random process as a result of which the theoretical spectrum of an oscillator signal  $v(t)$  is not defined. Additionally a theoretical spectrum is an ensemble property of a random process and can never be observed. Only sample functions of the random process are observable. A spectrum analyzer measures an approximation to an oscillator signal's theoretical spectrum [6]. The shape of the RF spectrum in the presence of white frequency noise only is given by a Lorentzian function [13]. However, in the presence of both white frequency and flicker of frequency noise, the shape of the RF spectrum is defined by a Voigt profile approximated by the convolution of a Gaussian and Lorentzian function [16].

SPICE simulation is used to estimate the constants for a 2.4-GHz 75- $\mu$ W ring oscillator ( $c = 0.5$  fs,  $c_F = 50$  ps) and a 2.4-GHz 240- $\mu$ W LC oscillator ( $c = 1.35$  as,  $c_F = 0.2$  fs), both designed in a 65 nm CMOS process excluding power supply noise and layout parasitics. A white-noise-only (i.e., no flicker noise) SPICE simulation is setup to calculate the spot RF spectral density for estimating  $c$  from a Lorentzian function which for small  $c$  and  $\Delta f$  is given by [13]

$$L(\Delta f) \approx \frac{f_o^2 c}{\pi^2 f_o^4 c^2 + \Delta f^2}. \quad (11)$$

A white and flicker noise SPICE simulation is setup to calculate the RF spectral density and the constant  $c_F$  is estimated through empirical curve fitting in MATLAB. Equations (7)–(9) are used to model the free-running oscillator PN in discrete time and the resulting spectrum is shown in Fig. 4 along with the RF spectrum obtained from analog fast SPICE PN simulation using the foundry models. The simulated discrete time PN accurately captures the free-running oscillator behavior.

The MATLAB source code to model the White and Flicker of frequency noise of a free running oscillator is hosted on a repository [17].

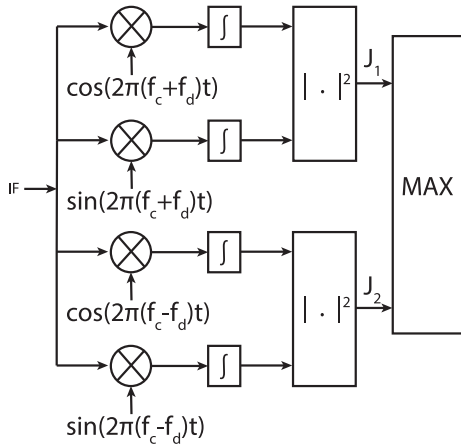


Fig. 5. Optimal incoherent MSK receiver [20].

### III. COMMUNICATION SYSTEM PERFORMANCE

The LO PN impacts communication system performance through: 1) additive noise; 2) spectral spreading; 3) coherence loss; and 4) reciprocal mixing [18]. When the desired RF channel is mixed with a noisy LO, the PN appears as noise added to the desired signal, which decreases the signal-to-noise ratio (SNR). Spectral spreading refers to when PN spreads the signal energy of a modulated signal in the frequency domain resulting in decreased SNR due to a loss of signal energy. The coherence loss is associated with coherent receivers that use the noisy LO in a PLL to estimate the phase of the incoming carrier signal. The resulting carrier phase estimate accuracy is limited due to the LO PN and is categorized as loss in performance due to coherence error. Finally, the noisy LO skirts in the frequency domain due to PN mix with unwanted interferers and cause the mixing terms to fall in-band that degrades the system SNR, which is referred to as reciprocal mixing.

We evaluate the impact of PN on the performance of an incoherent receiver for the additive noise and spectral spreading loss. The coherence loss is not applicable and the reciprocal mixing, which specifies the blocking performance of a receiver, is not considered in this brief.

The IEEE 802.15.4 standard uses OQPSK modulation with half-sine pulse shaping (HSS) in the 2.4-GHz ISM band. The OQPSK-HSS is equivalent to minimum shift keying (MSK) modulation and can thus be demodulated in the same manner as MSK [19]. Fig. 5 shows the block diagram of the optimal incoherent MSK envelope detector used for demodulation [20].

A discrete time simulation model of Fig. 2 was developed in MATLAB using a free running LC/ring oscillator as an LO for down-conversion to the intermediate frequency (IF). An ideal 1-bit ADC is used to quantize the signal and square wave templates are used instead of sinusoidal templates for the incoherent matched filter (MF). This choice results in a simplified hardware implementation at the expense of slightly reduced performance.

The IEEE 802.15.4 standard uses direct sequence spread spectrum coding to mitigate RF channel impairments. The chip error rate (Pce) using the matched filter of Fig. 5 is plotted

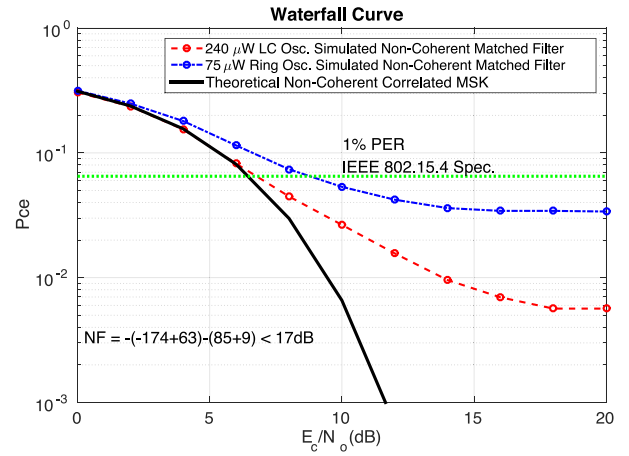


Fig. 6. Waterfall curve for MSK signaling with LO PN.

in Fig. 6. The horizontal line specifies the required chip error rate (6.5%) to meet the 1% packet error rate (PER) standard specification [21]. Since the MSK tone spacing is half of the data rate, the two MSK tones are correlated (nonorthogonal) for incoherent detection [19]. The simulated chip error probability (Pce) is compared with the theoretical performance of the incoherent correlated MSK. The correlation coefficient  $\rho$  is computed empirically to be 0.3. The probability of chip error is given by [19]

$$P_b = Q_1(a, b) - \frac{1}{2} e^{-\frac{E_c}{2N_o}} I_0\left(\frac{E_c}{2N_o} |\rho|\right)$$

$$a = \sqrt{\frac{E_c}{2N_o} \left(1 - \sqrt{1 - |\rho|^2}\right)}$$

$$b = \sqrt{\frac{E_c}{2N_o} \left(1 + \sqrt{1 - |\rho|^2}\right)} \quad (12)$$

where  $E_c$  is the energy per chip,  $N_o$  is the one-sided noise spectral density,  $Q_1(a, b)$  is the Marcum  $Q$  function, and  $I_0(x)$  is the modified Bessel function of order zero. The simulated Pce levels-off at high SNR to about 3.4% chip error rate due to the ring LO PN and to about 0.6% for the LC LO PN, which limits the equivalent SNR to about  $\sim 8$  and  $\sim 10$  dB, respectively.

### IV. DISCUSSION

It is shown that a frequency-calibrated free-running oscillator used as an LO can meet the IEEE 802.15.4 1% PER requirement in an AWGN channel. For the simulated PN profile of a 2.4-GHz 75- $\mu$ W ring oscillator, this corresponds to a noise figure (NF) specification of less than 17 dB for the incoherent receiver (1-bit ADC with square templates for the MF). To the authors' best knowledge, this is the first paper clearly specifying the NF requirement of a radio receiver exploiting a free-running LO. The noise performance of an RF front-end and the PN of an oscillator both trade with power. The RF sensitivity of  $-85$  dBm (NF of less than 17 dB) can be achieved with a low-noise amplifier consuming about 100  $\mu$ W and 1–2 mW should improve the sensitivity to  $-95$  dBm (NF less than 7 dB), which



is comparable to many commercial products, and with about 10 mW and NF = 1 dB, the sensitivity of a crystal-free receiver could be pushed to  $-101$  dBm [22].

Contrary to conventional wisdom, the close-to-carrier PN of a frequency-calibrated free-running LO does not actually affect the best-case sensitivity of a well-designed receiver by more than a few decibels. Accurately quantifying the impact of a given oscillator's PN profile on the wireless communication system performance allows an RF designer to optimize the power of an oscillator as well as for the radio front-end. This results in significant power savings by avoiding excessive design margins for energy autonomous millimeter-scale microsystems.

## REFERENCES

- [1] M. H. Roshan *et al.*, "11.1 Dual-MEMS-resonator temperature-to-digital converter with 40 K resolution and FOM of 0.12pJK<sup>2</sup>," in *Proc. Int. Solid State Circuits Conf. (ISSCC)*, San Francisco, CA, USA, 2016, pp. 200–201.
- [2] S. Zaliasl *et al.*, "A 3 ppm 1.5 × 0.8 mm 2 1.0 μA 32.768 kHz MEMS-based oscillator," *IEEE J. Solid-State Circuits*, vol. 50, no. 1, pp. 291–302, Jan. 2015.
- [3] Y.-C. Shih and B. Otis, "An on-chip tunable frequency generator for crystal-less low-power WBAN radio," *IEEE Trans. Circuits Syst. II, Exp. Briefs*, vol. 60, no. 4, pp. 187–191, Apr. 2013.
- [4] X. Zhang, I. Mukhopadhyay, R. Dokania, and A. B. Apsel, "A 46-μW self-calibrated gigahertz VCO for low-power radios," *IEEE Trans. Circuits Syst. II, Exp. Briefs*, vol. 58, no. 12, pp. 847–851, Dec. 2011.
- [5] O. Khan *et al.*, "Frequency reference for crystal free radio," in *Proc. Int. Freq. Control Symp.*, New Orleans, LA, USA, 2016, pp. 1–2.
- [6] F. M. Gardner, *Phaselock Techniques*, 3rd ed. Hoboken, NJ, USA: Wiley, 2005.
- [7] D. A. Howe, "Frequency domain stability measurements: A tutorial introduction," Nat. Bureau Standards, Time Frequency Divis., Inst. Basic Standards, Boulder, CO, USA, NASA STI/Recon Tech. Rep. 76, Mar. 1976.
- [8] F. L. Walls and D. W. Allan, "Measurements of frequency stability," *Proc. IEEE*, vol. 74, no. 1, pp. 162–168, Jan. 1986.
- [9] D. W. Allan, "The measurement of frequency and frequency stability of precision oscillators," Time Frequency Divis., Inst. Basic Standards, Nat. Bureau Standards, Boulder, CO, USA, May 1975.
- [10] W. P. Robins, *Phase Noise in Signal Sources*. Stevenage, U.K.: Inst. Eng. Technol., Dec. 1983.
- [11] S. Bittner, S. Krone, and G. Fettweis. *Tutorial on Discrete Time Phase Noise Modeling for Phase Locked Loops*. [Online]. Available: <http://www.vodafone-chair.com/staff/bittner/>
- [12] D. C. Lee, "Modeling timing jitter in oscillators," in *Proc. Forum Design Lang.*, Lyon, France, Sep. 2001.
- [13] A. Demir, A. Mehrotra, and J. Roychowdhury, "Phase noise in oscillators: A unifying theory and numerical methods for characterization," *IEEE Trans. Circuits Syst. I, Fundam. Theory Appl.*, vol. 47, no. 5, pp. 655–674, May 2000.
- [14] N. J. Kasdin and T. Walter, "Discrete simulation of power law noise," in *Proc. Freq. Control Symp.*, vol. 46. Hershey, PA, USA, Jun. 1992, pp. 274–283.
- [15] J. R. M. Hosking, "Fractional differencing," *Biometrika*, vol. 68, no. 1, pp. 165–176, 1981.
- [16] L. B. Mercer, "1/f frequency noise effects on self-heterodyne linewidth measurements," *J. Lightw. Technol.*, vol. 9, no. 4, pp. 485–493, Apr. 1991.
- [17] O. Khan. *Free Running Oscillator*. Accessed on Aug. 26, 2016. [Online]. Available: <https://github.com/openwsn-berkeley/free-running-oscillator/blob/master/free-running-oscillator.m>
- [18] R. P. Gilmore, "Specifying local oscillator phase noise performance: How good is good enough?" in *Proc. IEEE Int. Symp. Pers. Indoor Mobile Radio Commun.*, Sep. 1991, pp. 166–172.
- [19] J. G. Proakis and M. Salehi, *Digital Communications*, 5th ed. New York, NY, USA: McGraw-Hill, 2014.
- [20] J. R. Barry, E. A. Lee, and D. G. Messerschmitt, *Digital Communication*, 3rd ed. New York, NY, USA: Springer, 2004.
- [21] S. Lanzisera and K. S. J. Pister, "Theoretical and practical limits to sensitivity in IEEE 802.15.4 receivers," in *Proc. 14th IEEE Int. Conf. Electron. Circuits Syst.*, Marrakesh, Morocco, 2007, pp. 1344–1347.
- [22] O. U. Khan and D. D. Wentzloff, "8.1 nJ/b 2.4 GHz short-range communication receiver in 65 nm CMOS," *IEEE Trans. Circuits Syst. I, Reg. Papers*, vol. 62, no. 7, pp. 1854–1862, Jul. 2015.